© 2023. Published by The Company of Biologists Ltd | Journal of Cell Science (2023) 136, jcs260000. doi:10.1242/jcs.260000

TOOLS AND RESOURCES

A CRISPR-del-based pipeline for complete gene knockout in human diploid cells

Takuma Komori[1,*], Shoji Hata[1,2,*,‡], Akira Mabuchi[1], Mariya Genova[3], Tomoki Harada[1], Masamitsu Fukuyama[1], Takumi Chinen[1] and Daiju Kitagawa[1,‡]

ABSTRACT

The advance of CRISPR/Cas9 technology has enabled us easily to generate gene knockout cell lines by introducing insertion–deletion mutations (indels) at the target site via the error-prone non-homologous end joining repair system. Frameshift-promoting indels can disrupt gene functions by generation of a premature stop codon. However, there is growing evidence that targeted genes are not always knocked out by the indel-based gene disruption. Here, we established a pipeline of CRISPR-del, which induces a large chromosomal deletion by cutting two different target sites, to perform 'complete' gene knockout efficiently in human diploid cells. Quantitative analyses show that the frequency of gene deletion with this approach is much higher than that of conventional CRISPR-del methods. The lengths of the deleted genomic regions demonstrated in this study are longer than those of 95% of the human protein-coding genes. Furthermore, the pipeline enabled the generation of a model cell line having a bi-allelic cancer-associated chromosomal deletion. Overall, these data lead us to propose that the CRISPR-del pipeline is an efficient and practical approach for producing 'complete' gene knockout cell lines in human diploid cells.

KEY WORDS: CRISPR/Cas9, Complete gene knockout, CRISPR-del

INTRODUCTION

Gene knockout is a powerful technique for studying gene functions in experimental biology. Recent advances in genome editing technology have enabled us to conduct the gene knockout approach efficiently in a variety of organisms and cultured cells (Doudna and Charpentier, 2014; Hsu et al., 2014). Among the currently available genome editing tools, the CRISPR/Cas9 system, derived from the adaptive immune system of prokaryotes, is the most widely used tool for gene knockout. The CRISPR-associated protein Cas9 is an RNA-guided endonuclease that induces double-strand breaks (DSBs) at specific DNA loci (Jinek et al., 2012). These DSBs can be repaired via the efficient but error-prone non-homologous end joining (NHEJ) pathway, which frequently introduces small insertion–deletion mutations (indels) at the junction sites (Chang et al., 2017; Rouet et al., 1994). Frameshift-promoting indels generate premature termination codons (PTCs) downstream of the target site, leading to nonsense-mediated decay of the transcript or production of a nonfunctional truncated protein (Popp and Maquat, 2016).

Most of the widely applied approaches for CRISPR/Cas9-mediated gene disruption rely on the introduction of indels after DSB (Ran et al., 2013; Shalem et al., 2015), although there is accumulating evidence that this method does not always ensure a complete gene knockout. For example, Bub1, a spindle assembly checkpoint kinase, is known to be a 'zombie' protein, which remains functional despite the presence of CRISPR/Cas9-generated indels (Meraldi, 2019; Rodriguez-Rodriguez et al., 2018; Zhang et al., 2019). Recent studies demonstrate that Bub1 'knockout' clones express alternatively spliced Bub1 mRNA (Rodriguez-Rodriguez et al., 2018) or low levels of an active Bub1 mutant harboring a small deletion (Zhang et al., 2019). Similarly, nonsense-associated altered splicing enables skipping of the exon harboring a PTC, thus allowing the production of functional proteins (Bagheri et al., 2022; Mou et al., 2017; Tuladhar et al., 2019). In addition to the altered splicing, alternative translation initiation is another often observed phenomenon in mutant clones generated by the indel-based method (Tuladhar et al., 2019). Several mechanisms, such as leaky scanning and internal ribosome entry, allow translation to start from an alternative initiation site on the edited transcript, in order to evade gene disruption caused by PTCs (Xu et al., 2020). Owing to these cellular abilities to bypass PTCs, the indel-based method is not always the optimal strategy to achieve complete gene knockout.

By contrast, the CRISPR/Cas9 deletion (CRISPR-del) is an alternative approach that can be applied to unambiguously disrupt a gene of interest (Canver et al., 2014; Raaijmakers and Medema, 2019; Xiao et al., 2013). CRISPR-del uses Cas9 and two different single guide RNAs (sgRNAs) to delete a large chromosomal region flanked by the two target sequences, thus ensuring a complete gene knockout. However, the efficiency of chromosomal deletions by CRISPR-del and the feasible deletion length in routine lab work have not been thoroughly investigated, especially in chromosomally stable human diploid cells.

In this study, we developed a pipeline of CRISPR-del for the use in systematic gene knockout in human cell lines with a near-diploid karyotype. Two different quantitative analyses show that our CRISPR-del strategy is more efficient than previous CRISPR-del methods and is capable of deleting a very long region of genomic DNA. The length covers that of more than 95% of human protein-coding genes. Furthermore, the CRISPR-del method can be used to create model human cell lines with cancer-associated large

[1]Department of Physiological Chemistry, Graduate School of Pharmaceutical Sciences, The University of Tokyo, Bunkyo, 113-0033 Tokyo, Japan. [2]Precursory Research for Embryonic Science and Technology (PRESTO) Program, Japan Science and Technology Agency, Honcho Kawaguchi, 102-8666 Saitama, Japan. [3]Zentrum für Molekulare Biologie, Universität Heidelberg, DKFZ-ZMBH Allianz, 69120 Heidelberg, Germany.
*These authors contributed equally to this work

‡Authors for correspondence (s.hata@mol.f.u-tokyo.ac.jp; dkitagawa@mol.f.u-tokyo.ac.jp)

S.H., 0000-0003-4094-0489; D.K., 0000-0003-2509-5977

Handling Editor: David Glover
Received 7 March 2022; Accepted 2 February 2023

Journal of Cell Science (2023) 136, jcs260000. doi:10.1242/jcs.260000

chromosomal deletions identified in patients. Taken together, this study leads us to propose that the CRISPR-del pipeline can efficiently generate complete gene knockout cell lines in human diploid cells.

RESULTS

An optimized CRISPR-del pipeline is a practical approach with increased throughput for gene knockout in human diploid cells

In order to increase throughput of CRISPR-del for producing gene knockout cell lines in human diploid cells, we first optimized several steps in the conventional method of CRISPR-del (Canver et al., 2014) in the hTERT-immortalized RPE1 cell line, which is one of the most widely used human diploid cell lines (Fig. 1A). To avoid the construction of sgRNA plasmids, which can be time consuming, sgRNAs were synthesized via *in vitro* transcription from PCR-assembled DNA templates. We generally designed two different sgRNAs for each upstream and downstream target site flanking a deletion region, having four different combinations of sgRNA pairs. Each sgRNA pair was mixed with commercially available recombinant Cas9 protein, and the ribonucleoprotein (RNP) complexes were electroporated into RPE1 cells under an optimized condition. Delivery of CRISPR RNP via electroporation is known to be the most robust method in terms of editing efficiency and minimized off-target effects (Kim et al., 2014; Liang et al., 2015). After recovery from electroporation and genome editing, the deletion efficiency of each sgRNA pair was promptly analyzed by genomic PCR with primers designed to detect the expected deletion. From the cell pool of the sgRNA pair with the highest deletion efficiency, single cells were isolated into 96-well plates. The use of an automated single-cell-dispensing system based on piezo-acoustic technology resulted in a reliable clone isolation with high viability. After expansion for ∼3 weeks in culture, each cell colony was detached from its well with trypsin-EDTA solution and split into two new 96-well plates. For one of them, the cells were cultured in normal medium and then subjected for genomic DNA extraction directly in the plate. In case of long-term storage of the other replicated plate, the detached cells in trypsin-EDTA solution were directly mixed with three times volume of a DMSO-free cryopreservation medium, and the plate was placed and stored in a −80°C freezer. This procedure allows for genotyping analysis and cell expansion from the replicated plate at flexible timing. Two types of genotyping PCRs were conducted with the extracted DNA by using primers to detect either the wild-type (WT) or the deleted allele in a high-throughput manner for the whole plate. The PCR products were automatically analyzed by a microtip electrophoresis system to identify bi-allelic knockout clones showing an expected pattern of a deletion band and the absence of a WT band. Knockout clones were then expanded from the replicated plate and subjected to a second genomic PCR using their purified genomic DNA to confirm the expected deletion in both alleles. In summary, our optimizations in several procedures enable CRISPR-del to become a method with increased throughput for generation of gene knockout cells.

To prove that our optimized CRISPR-del pipeline can be used for gene knockout in RPE1 cells, we applied it to target the *CEP128* gene, which encodes a centrosomal protein. The length of this gene is 502.54 kb, which is longer than 95% of the human protein-coding genes (Soheili-Nezhad, 2017 preprint). We first designed two sgRNAs (named as CEP128 sgRNA#1 and #2) to delete a 20-kb region ranging from 35 bp downstream of the first ATG in exon 3 to the middle of intron 8 of the longest CEP128 transcript variant (NM_152446) (Fig. 1B). Electroporation of Cas9 protein with the combination of sgRNA#1 and #2, but not with each individual sgRNA, resulted in a successful chromosomal deletion (Fig. S1A). We then performed genotyping analysis of single-cell clones from the *CEP128*-deleted cell pool. Microtip electrophoresis analyses followed by direct genomic PCRs revealed one clone in which a deletion, but not a WT DNA band, was detected, suggesting both alleles of the gene were edited (Fig. 1C). Further genotyping using the purified genomic DNA of this clone confirmed the result, indicating that it has the expected 20-kb deletion in both *CEP128* alleles (Fig. 1D). Western blotting with an antibody against the CEP128 C-terminus region revealed that the full-length protein is not expressed in the mutant clone (Fig. 1E). Unexpectedly, smaller fragments recognized by the CEP128 antibody were specifically expressed in the 20-kb del clone. Given that the fragments disappeared upon CEP128 knockdown (Fig. S1B), we conclude that they are smaller CEP128 fragments that probably emerged due to alternative translation initiation or nonsense-associated altered splicing on the deleted CEP128 transcripts in the mutant clone. Nevertheless, the absence of both CEP128 and its downstream protein centriolin (Mazo et al., 2016) was confirmed at the centrosome of the clone by immunofluorescent analyses (Fig. 1F,G; Fig. S1C–E), indicating that the optimized CRISPR-del successfully knocked out the CEP128 gene in RPE1 cells.

To further verify whether this knockout pipeline is applicable for other genes and cell lines, we introduced a 27-kb deletion into the genomic locus of kinesin light chain 1 (*KLC1*) gene in a near-diploid human colorectal carcinoma cell line HCT116 in addition to RPE1 cells (Fig. S2A). Delivery of CRISPR RNP via electroporation resulted in much higher deletion efficiency of the targeted *KLC1* region compared to a lipofection method (Fig. S2B). The electroporated cells were then subjected to single-cell cloning. Genotyping analysis revealed that single-cell clones harboring the expected bi-allelic deletion of the *KLC1* gene were successfully generated for both RPE1 and HCT116 cell lines (Fig. S2C,D). We further confirmed the absence of KLC1 protein in a RPE1 clone with the bi-allelic deletion by immunofluorescent analysis (Fig. S2E). Taken together, these data indicate that the optimized CRISPR-del pipeline can be used for successful gene knockout in human diploid cells.

The CRISPR-del pipeline effectively generates a nearly complete, bi-allelic deletion of a large protein-coding gene

For the purpose of achieving complete gene knockout in human cells, it would be important to estimate the length of the genomic DNA that can be eliminated by the current genome editing technology. Accordingly, we analyzed what length and how frequently genomic deletions could be achieved in RPE1 cells with the CRISPR-del pipeline for routine laboratory work. Given that the full length of *CEP128* is 502.54 kb, we tried to introduce deletions larger than the successfully obtained 20-kb one. In combination with sgRNA#1 that targets the site around the first ATG in exon 3, two other sgRNAs were designed at the downstream end to delete 50 kb, 200 kb and 440 kb of the gene, respectively (Fig. 2A). For all deletions, the more effective one of the two sgRNAs was used in combination with sgRNA#1 to quantify their deletion frequencies (Fig. S3A,B). Single-cell clones from two 96-well plates were genotyped for all three conditions (Fig. S3C). In the case of the targeted 50-kb deletion, we found 132 (69.8%) and 6 (3.2%) clones harboring mono- and bi-allelic deletions, respectively, among 189 surviving clones (Fig. 2B). For 200-kb and 440-kb targeted deletions, the frequency of the mono-allelic

Journal of Cell Science (2023) 136, jcs260000. doi:10.1242/jcs.260000

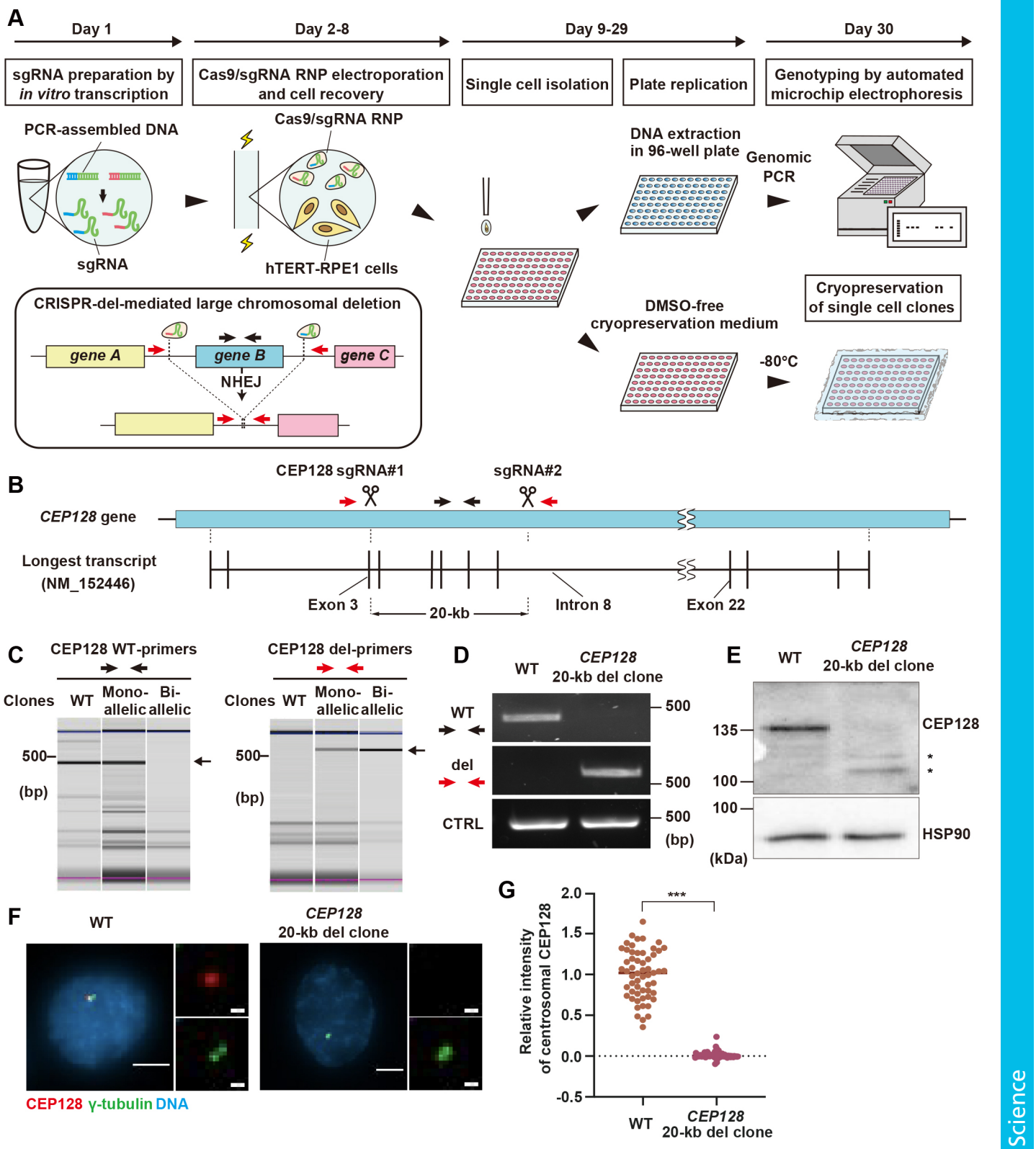

Fig. 1. See next page for legend.

deletion was calculated as 42.0% (74/176) and 26.6% (45/169), respectively. Even though the frequency of bi-allelic deletions was also reduced as the deletion length increased (200 kb; 5/176, 2.8%), 3 out of 169 clones (1.8%) were found to have the very long 440-kb deletion for both alleles. Considering the number of deleted alleles out of the total number of alleles of all analyzed clones combined, the deletion frequency for 50 kb, 200 kb and 440 kb were calculated to be 38.1%, 23.9%, 15.1%, respectively (Fig. 2B). The relationship between the length and the frequency of chromosomal deletion was an inverse correlation (Fig. 2C). Compared to the mono-allelic

Journal of Cell Science (2023) 136, jcs260000. doi:10.1242/jcs.260000

Fig. 1. An optimized pipeline of CRISPR-del enables efficient gene knockout in human diploid RPE1 cells. (A) Schematic overview of the optimized high-throughput CRISPR-del method. Cas9/sgRNA complexes introduce a large deletion of a chromosomal region flanked by the two sgRNA target sequences. (B) Schematic representation of the *CEP128* gene and the longest transcript variant annotated in genome databases. The target positions of sgRNAs and the expected deletion length are shown. Black and red arrows indicate locations of primers to detect WT and the deleted region of *CEP128* gene, respectively. (C) Genomic PCR for detection of WT and the 20-kb deleted alleles of *CEP128* gene using the indicated primers, analyzed by the automated microchip electrophoresis system. Each electrophoresis pattern was adjusted according to the upper (blue) and lower (pink) size makers. The arrows on the side of electrophoresis images indicate the specific PCR product. The images are representative of one experiment to show the genotyping results analyzed by the automated microchip electrophoresis. (D) Genomic PCR as in C with purified genomic DNA, analyzed by agarose gel electrophoresis. (E) Western blotting to analyze the protein expression of CEP128 in WT cells and a *CEP128* 20-kb deleted clone. HSP90 was used as loading control. Asterisks show smaller fragments of CEP128 protein. Images shown in D,E are representative of three experimental repeats. (F) Immunofluorescence imaging of CEP128 and γ-tubulin in WT cells and the 20-kb deleted clone. Scale bars: 5 µm (1 µm for magnified views). (G) Quantification of relative CEP128 intensity at the centrosome from F, ≥50 cells each. The mean is shown. ***P<0.001 (Mann–Whitney U test).

deletions, the frequency of the bi-allelic deletions was very low in this experiment. This is not the case for KLC1, where the ratio of mono- and bi-allelic deletion frequencies was within the expected range (Fig. S2D). These data might indicate that the bi-allelic knockout of CEP128 reduces the proliferative ability of RPE1 cells due to the loss of an unknown function of CEP128. The genotype of the 440-kb deleted clones was confirmed by genomic PCR with the purified DNA (Fig. 2D) and subsequent genomic sequencing (Fig. 2E; Fig. S3D). Consistent with this, western blotting showed that the expression of CEP128 was abolished in these clones (Fig. 2F). Immunofluorescence microscopy further confirmed that the downstream protein centriolin was absent from the centrosome of the mutant clones (Fig. S1C,D). These analyses demonstrate that successful deletions were achieved for almost an entire locus in both *CEP128* alleles in RPE1 cells. In the human genome, more than 95% of the protein-coding sequences have a length shorter than the here demonstrated possible deletion of 440 kb (Soheili-Nezhad, 2017 preprint). Our data therefore indicate that most of the human genes could be completely deleted by the CRISPR-del pipeline.

A high-throughput quantification reveals that highly efficient large chromosomal deletions can be achieved by the optimized CRISPR-del

To further analyze the deletion efficiency in a high-throughput and quantitative manner, we engineered a mono-allelic knock-in cell line expressing a fluorescent protein and designed a FACS-based experimental system that can determine whether or not gene deletion has occurred based on the presence or absence of fluorescence. Using the CRISPR/Cpf1 system and a PCR-assembled dsDNA donor template, the nuclear ribonucleoprotein-coding *HNRNPA1* gene of RPE1 cells was targeted for endogenous tagging with mNeonGreen (mNG) at its C-terminus via homologous recombination (Fig. 3A). After genome editing, cells having mNG signal were subjected to single-cell cloning. By performing genomic PCR to detect both WT and the knock-in alleles, we established a mono-allelic *HNRNPA1-mNG* knock-in clone (Fig. S4A,B). Fluorescence imaging analysis confirmed a specific nuclear signal of mNG in this clone (Fig. S4C). To verify the quantification strategy, we first tried to remove a 20-kb region containing the mNG sequence inserted to the *HNRNPA1* gene. For this purpose, we designed the first sgRNA (named as sgRNA#0) to target a sequence in *NFE2*, which is upstream on chromosome 12 of *HNRNPA1*, and two versions of the second sgRNAs (named as sgRNA 20-kb#1 and #2) to target the intron 7 or 8 of *HNRNPA1* respectively (Fig. 3A; Fig. S4D). We then performed CRISPR-del in RPE1 *HNRNPA1-mNG* cells using these different combinations of sgRNAs. At 8 days after the electroporation, we found that the combination of sgRNA#0 with sgRNA 20-kb#2, but not with a non-specific control sgRNA (CTRL), resulted in the appearance of a certain number of cells with undetectable mNG signal in the nucleus (Fig. 3B). For high-throughput quantification of the gene deletion efficiency, the RPE1 *HNRNPA1-mNG* cells subjected to CRISPR-del were analyzed for fluorescent signal by a high-content flow cytometer. The electroporation of sgRNA 20-kb#1 and #2, in combination with sgRNA#0, produced 4.9±0.3% and 14.8%±0.2% (mean±s.d.) of mNG-negative cells, respectively (Fig. 3C,D). Given that HNRNPA1 is an abundant protein due to its strong housekeeping promoter (Biamonti et al., 1993), most of the cells without mNG signal likely have the deletion of the target region.

We further analyzed the gene deletion efficiency for much longer genomic regions by the optimized CRISPR-del. To avoid closed chromatin regions, second sgRNAs were designed to target sequences within genes downstream of *HNRNPA1* on the chromosome. The second sgRNAs were for the deletion of 50 kb, 110 kb, 590 kb and 1000 kb targeted to the *CBX5*, *SMUG1*, *CALCOCO1* and *MYG1* genes, respectively. In combination with the first sgRNA#0, the effect of each second sgRNA on gene deletion efficiency was quantitatively analyzed as mentioned above. Despite the variable results among the sgRNA combinations, at least one of the two combinations significantly increased the percentage of mNG-negative cells, compared to the control (Fig. 3E,F). To test the possibility that the different frequency in the generation of mNG-negative cells between the two sgRNAs was due to the cutting efficiency of the sgRNA, we performed the T7E1 mismatch cleavage assay. In this assay, more digested DNA bands were detected in the sgRNAs with higher deletion rates (Fig. S4E), suggesting that the efficiency of CRISPR-del is positively correlated with the cutting efficiency of individual sgRNAs. Surprisingly, an increase of mNG-negative cells to 5.8±1.0% (mean±s.d.) was observed with a sgRNA combination targeting a very long 1000-kb deletion. By genomic PCR (Fig. S4D,F) and subsequent genomic sequencing (Fig. S4G), the occurrence of the 1000-kb deletion was confirmed in the purified DNA from the cells electroporated with Cas9 and the sgRNA pair. It should be noted that the percentage of mNG-negative cells in this experiment might be under- or over-estimated if genomic loci critical for cell proliferation are present in the large target regions. Collectively, these quantitative analyses revealed that, using effective sgRNA pairs, our optimized CRISPR-del enables deletion of a large chromosome region in RPE1 cells at high frequency.

The optimized CRISPR-del can introduce a homozygous deletion of cancer-associated large genomic regions into human diploid cells

Large chromosomal deletions are frequently observed in human cancers (Beroukhim et al., 2010; Bignell et al., 2010). To investigate the impact of chromosome deletions on the development and progression of cancers, it is important to create model cell lines bearing these cancer-associated heterozygous or homozygous deletions. The 9p21.3 region, which contains the three tumor

Journal of Cell Science (2023) 136, jcs260000. doi:10.1242/jcs.260000

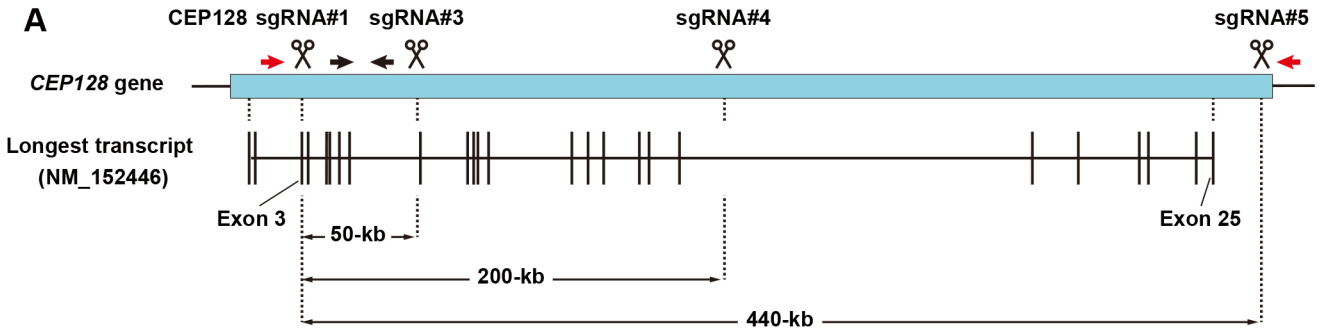

B

	Deletion length within *CEP128* gene		
	50-kb	200-kb	440-kb
Mono-allelic deleted clones	132/189 (69.8%)	74/176 (42.0%)	45/169 (26.6%)
Bi-allelic deleted clones	6/189 (3.2%)	5/176 (2.8%)	3/169 (1.8%)
Deletion Frequency	38.1%	23.9%	15.1%

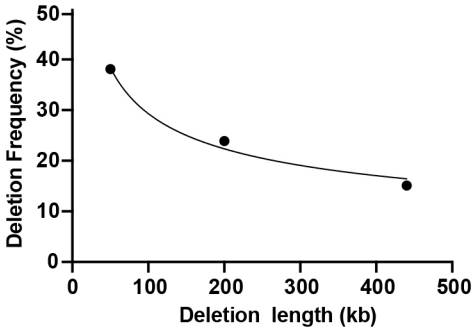

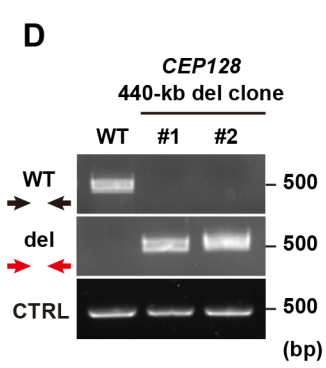

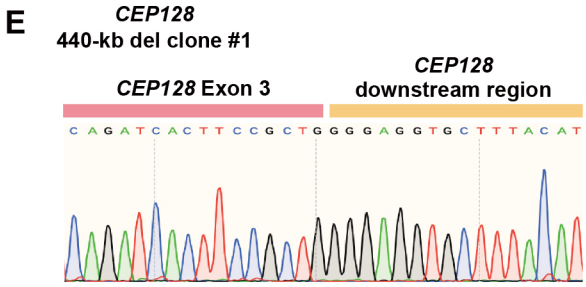

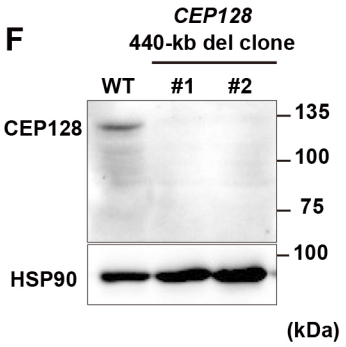

Fig. 2. Analysis of efficacy in mono- and bi-allelic gene knockouts with a variety of deletion lengths using the CRISPR-del pipeline. (A) Schematic representation of the *CEP128* gene and the longest transcript variant annotated in genome databases. The target positions of sgRNAs and the expected lengths of large deletions are shown. Black and red arrows indicate locations of primers to detect WT and the deleted regions, respectively. (B) Summary for the efficiency of mono- and bi-allelic deletions within *CEP128* gene. (C) A graph showing a relationship between the length and the frequency of chromosomal deletion from C. (D) Genomic PCR for detection of WT and the 440-kb deleted alleles of *CEP128* gene using the indicated primers. (E) Sequencing result of the CEP128 deleted alleles in the 440-kb deleted clone #1. (F) Western blotting to analyze the protein expression of CEP128 in the lysate of WT cells and the 440-kb deleted clones. HSP90 was used as loading control. Images shown in D,F are representative of three experimental repeats. The experiment in E was performed once as it shows the result of DNA sequencing, and the possibility that it might change with the number of trials was not considered.

suppressor genes *CDKN2A*, *CDKN2B* and *MTAP*, is known to be frequently deleted in different types of cancer cells (Baker et al., 2016; Frigerio et al., 2014; Sasaki et al., 2003). Especially in bladder cancer cell lines, this region is commonly lost, and the deletions are extended to the genes located upstream and downstream of the tumor suppressors (Nickerson et al., 2017). Therefore, we tested whether the optimized CRISPR-del can introduce a homozygous deletion that is similar to that identified in the bladder cancer cell line UM-UC-3 (Nickerson et al., 2017) into the genome of non-transformed RPE1 cells (Fig. 4A). To delete the 650-kb region in chromosome 9, first and second sgRNAs were designed to target an upstream sequence of *MTAP* and a downstream sequence of *DMRTA1*. After CRISPR-del editing followed by single-cell cloning, genotyping was performed using different primer pairs to detect the four individual genes in the region. We identified a clone lacking all four genes (Fig. 4B) and showing a specific PCR product indicating the expected large deletion (Fig. 4C). Western blotting confirmed that p15, a protein encoded by *CDKN2B*, was not expressed in the 9p21.3 large deletion clone (Fig. 4D). These results demonstrate that our optimized CRISPR-del pipeline can be applied for the generation of model cell lines with cancer-associated large chromosomal deletions in a non-transformed human diploid cell background.

DISCUSSION

The indel-based gene editing via the CRISPR/Cas9 technology is a well-established method for a simple, easy and cost-effective gene disruption, as compared to previous genome editing techniques.

Journal of Cell Science (2023) 136, jcs260000. doi:10.1242/jcs.260000

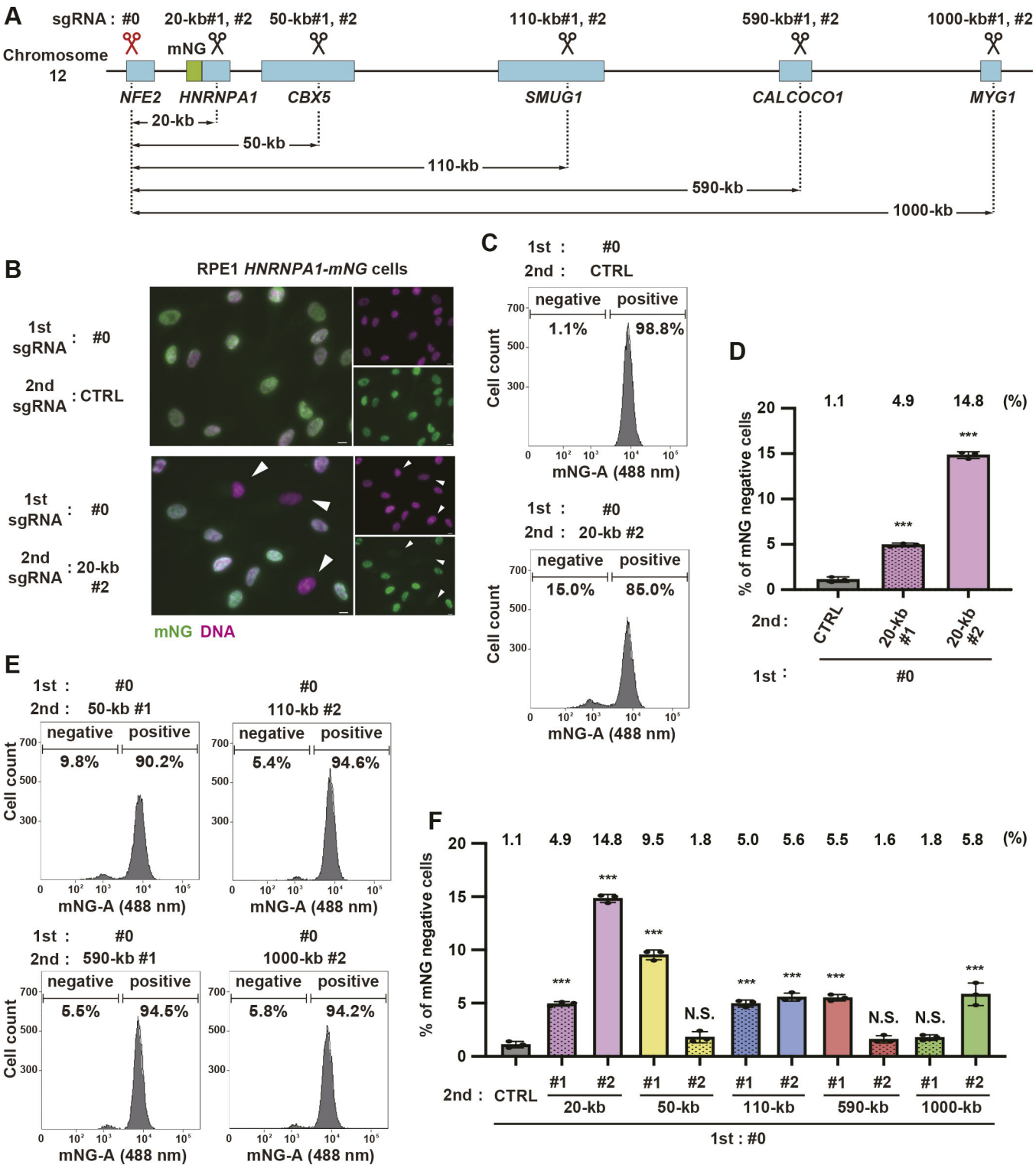

Fig. 3. Quantitative analyses of length-dependent DNA deletion efficiency for the optimized CRISPR-del method using flow cytometry.
(A) Schematic representation of the chromosome region around the *HNRNPA1* gene locus. The mNG tag was inserted into the chromosomal site at the C-terminus of *HNRNPA1* gene. The target positions of sgRNAs and the expected lengths of large deletions are shown. (B) Fluorescence imaging of HNRNPA1–mNG in RPE1 *HNRNPA1-mNG* cells electroporated with Cas9 protein and the indicated sgRNA pairs. Images are representative of three experimental repeats. Arrowheads indicate cells without the expression of HNRNPA1–mNG. Scale bars: 10 µm. (C) FACS analyses for the mNG expression in RPE1 *HNRNPA1-mNG* cells electroporated with the indicated sgRNAs as in B. Cells at 8 days after Cas9/sgRNAs electroporation were analyzed. (D) Quantification of mNG negative cells for each sgRNA pair from C. *N*=three biologically independent samples. ≥10,000 cells were analyzed for each sample. The percentage of mNG-negative cells for each sample is indicated on top of the histogram. (E) FACS analyses with the indicated conditions, as in C. (F) Quantification of E, as in D. Data are represented as mean±s.d. **P*<0.05; ***P*<0.01; ****P*<0.001; N.S., not significant (Tukey–Kramer test).

Journal of Cell Science (2023) 136, jcs260000. doi:10.1242/jcs.260000

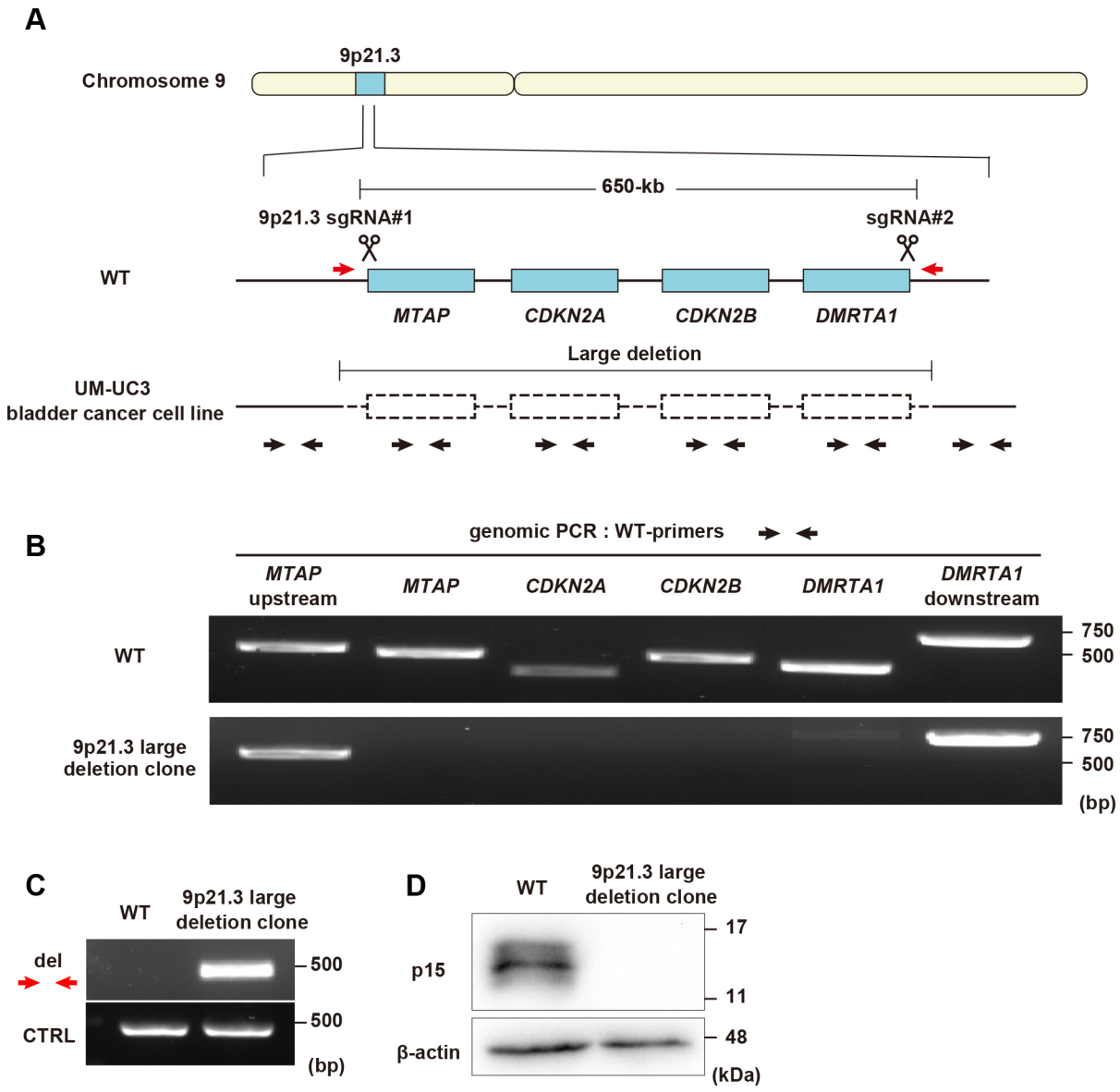

Fig. 4. Mimicking a cancer-associated large chromosome deletion by using the CRISPR-del pipeline in non-transformed human cells. (A) Schematic representation of the chromosome 9p21.3 region in the human genome. The UM-UC-3 bladder cancer cell line intrinsically has a large deletion containing the *MTAP*, *CDKN2A*, *CDKN2B* and *DMRTA1* genes. The target positions of sgRNAs are shown. Black and red arrows indicate locations of primers to detect WT and deleted genomic regions, respectively. (B) Genomic PCR for detection of the indicated regions within 9p21.3 in WT cells and a 9p21.3 large deletion clone. (C) Genomic PCR for detection of the large deletion in WT cells and the 9p21.3 large deletion clone. (D) Western blotting to analyze the protein expression of p15, the *CDKN2B* gene product, in WT cells and the deletion clone. β-actin was used as loading control. Images shown in B–D are representative of two experimental repeats.

Despite its wide usage and benefits, this method is not so reliable for 'complete' gene knockout, as several mechanisms can function to nullify the effects of indels. In this study, we established a pipeline of CRISPR-del, which can overcome the drawbacks of the indel-based method by removing an entire gene locus, for effective use in chromosomally stable human diploid cell lines.

Although the indel-based gene disruption is considered a generally simple method, the genotyping procedure for selecting knockout clones is time consuming and labor intensive due to the necessity for detection of these short indels. On top of that, the standard assays for the indel detection, such as the sequencing of genomic PCR products and the Surveyor assay using a mismatch specific nuclease, are costly. In contrast, the genotyping for CRISPR-del consists only of the preparation of genomic PCRs for detection of the WT and deleted alleles. In addition to this simple and cost-effective genotyping, our optimized pipeline of CRISPR-del includes several other fine-tuned steps: (1) the synthesis of sgRNAs from PCR-assembled DNA templates by *in vitro* transcription enables a cloning-free genome editing; (2) the electroporation of Cas9/sgRNA RNPs gives high editing efficiency with low off-target effects; (3) the use of an automated single-cell dispensing system based on piezo-acoustic technology provides an efficient single-cell cloning with high viability; (4) DMSO-free cryopreservation medium allows for a direct and mild freezing of cells in 96-well plates without removing cell dissociation solution; (5) the genomic DNA is directly extracted from single-cell clones in 96-well plates for genotyping PCR, and (6) the PCR products are automatically analyzed by a microtip

Journal of Cell Science (2023) 136, jcs260000. doi:10.1242/jcs.260000

electrophoresis system. These optimizations improve the CRISPR-del approach in terms of efficacy and cost, and allow for it to be implemented in high-throughput gene knockout studies of human diploid cells.

CRISPR-del has been considered to be a technique with a relatively low probability of successful knockout, as it was previously reported that 65% of sgRNA combinations yield deletion efficiency of <20% (Canver et al., 2014). However, in this study we implement optimizations to the method that demonstrates a much higher deletion rate. Quantitative analyses revealed that the optimized method successfully deleted chromosomal regions of 50 kb, 200 kb and 440 kb with 38.1%, 23.9%, and 15.1% efficiency, respectively. Although a fair comparison of the deletion efficiency between our approach and that of the previously described CRISPR-del methods is difficult due to the different quantitative analyses performed (He et al., 2015; Li et al., 2021), the study by Canver et al. calculated this factor in a similar manner (Canver et al., 2014). The authors conducted CRISPR-del in murine erythroleukemia cells, which led to chromosomal deletions of 20 kb, 71 kb and 1026 kb, with deletion efficiencies of 24.3%, 0.3% and 0.7%, respectively (Canver et al., 2014). Despite the poor transfectability of RPE1 cells, we demonstrate that our optimizations have dramatically improved CRISPR-del, rendering it a more effective method for large chromosomal deletions.

Based on the past experiments using CRISPR-del, the correlation between size and frequency of targeted chromosomal deletions seems to be controversial (Canver et al., 2014; He et al., 2015; Li et al., 2021). Our quantitative analyses show an inverse relationship between these parameters, which is similar to what was shown in the previous report (Canver et al., 2014). Although the length of the chromosomal deletion that can be introduced is a critical factor in performing a 'complete' gene knockout by CRISPR-del, our optimized method successfully achieved deletions of very long regions of genomic DNA: 440 kb for the *CEP128* gene, 1000 kb for the region around the *HNRNPA1* gene and 650 kb for the chromosomal region 9p21.3. This range covers the length of more than 95% of the human genes that encode proteins (Soheili-Nezhad, 2017 preprint), indicating that the CRISPR-del pipeline can be used to generate 'complete' knockout cell lines for most of the human protein-coding genes as routine laboratory work.

MATERIALS AND METHODS

Cell culture

RPE1 cells stably expressing Tet3G transactivator (Hata et al., 2019) (described as 'RPE1 cells' or 'RPE1 WT cells' in this study) and HCT116 cells obtained from the American Type Culture Collection (ATCC) were grown in Dulbecco's modified Eagle's medium F-12 (DMEM/F-12) and McCoy's 5A medium, respectively, together with 10% FBS, L-glutamine and penicillin-streptomycin. Cell culture reagents were sourced from Nacalai tesque. All cell lines were cultured at 37°C in a humidified 5% CO_2 incubator.

sgRNA synthesis

sgRNAs were designed using CRISPOR (Concordet and Haeussler, 2018) and Custom Alt-R® CRISPR-Cas9 guide RNA (IDT). sgRNAs were transcribed *in vitro* from PCR-generated DNA templates according to a previously published method (DeWitt et al., 2016) with slight modifications. Briefly, template DNA was assembled by PCR from five different primers: (1) a variable forward primer containing the T7 promoter and desired guide sequence, (2) a variable reverse primer containing the reverse complement of the guide sequence and the first 15 nt of the non-variable region of the sgRNA, (3) a forward primer containing the entire invariant region of the sgRNA, and (4,5) two amplification primers. The assembled template was purified and subjected to *in vitro* transcription by T7 RNA polymerase using the HiScribe T7 High Yield RNA Synthesis Kit (New England Biolabs). The reaction product was treated with DNase I, and the synthesized sgRNA was purified using the RNA Clean & Concentrator Kit (ZYMO RESEARCH). All sgRNA and primer sequences used in this study are listed in Tables S1 and S2, respectively.

CRISPR-del-mediated gene knockout

For large chromosomal deletions, the CRISPR-del method was performed with Cas9 protein and two synthesized sgRNAs. Cas9/sgRNA RNPs were electroporated into cells using the Neon Transfection System (Thermo Fischer Scientific) or Lipofectamine CRISPRMAX (Thermo Fisher Scientific) according to the manufacturer's protocol. Briefly, in electroporation, HiFi Cas9 protein (1.55 µM) from IDT and two sgRNAs (0.92 µM each) were pre-incubated in Resuspension buffer R and mixed with cells (0.125×10^5 cells/µl) and Cas9 electroporation enhancer (1.8 µM, IDT). After resuspension, electroporation was immediately conducted using a 10 µl Neon tip at a voltage of 1300 V with two 20 ms pulses for RPE1 cells, and 1200 V with one 40 ms pulse for HCT116 cells. The transfected cells were seeded into a 24-well plate. After recovery from the electroporation, single cells were isolated into 96-well plates using cellenONE (Cellenion) according to the manufacturer's protocol. After cell expansion, each 96-well plate was duplicated for genotyping and preparation of a frozen stock. Briefly, cells in 96-well plates were washed with PBS and treated with 25 µl of trypsin-EDTA solution (nacalai tesque). After brief incubation at 37°C, the detached cells were resuspended with 75 µl of Cell Reservoir One (nacalai tesque), a DMSO-free cryopreservation medium. 25 µl of the cell mixture was transferred into a well of another 96-well plate filled with 175 µl of growth medium for cell expansion followed by genotyping analysis. The 96-well plate with the remaining cell suspension was placed in a deep freezer at −80°C. For thawing frozen cells, the frozen 96-well plates were submerged in a water bath at 37°C. After thawing, the clones of interest were transferred into tubes containing fresh medium. After centrifugation (100 ***g*** for 2 min) and subsequent removal of supernatant, the cell pellet was resuspended with fresh medium and transferred into a new 96-well plate for culture.

Genotyping

For high-throughput genotyping, genomic DNA was directly extracted from single-cell clones in 96-well plates using DNAzol Direct (Molecular Research Center) and subjected to PCR for the detection of both WT and the deleted alleles using appropriate primers. Briefly, after removal of culture medium, 20 µl of DNAzol Direct was added to each well and the 96-well plate was shaken at 800 rpm for 20 min at room temperature. 1 µl of the lysate containing genomic DNA was used for 10 µl of PCR reaction using KOD One PCR Master Mix (TOYOBO). The PCR products were analyzed by the automated microchip electrophoresis system MCE-202 MultiNa (Shimadzu). To confirm the genotype of homozygous knockout clones, their genomic DNA was purified using NucleoSpin DNA RapidLyse kit (Macherey-Nagel) and subjected again to genotyping PCR. For a loading control, *NEK2* was used (labeled as CTRL). The PCR products were analyzed by agarose gel electrophoresis and sanger sequencing.

CRISPR/Cpf1-mediated gene knock-in

Endogenous mNG tagging of HNRNPA1 by the CRISPR/Cpf1 system was performed with the electroporation of Cpf1/crRNA RNP and dsDNA repair template. crRNA was designed to target the site immediately downstream of the stop codon of *HNRNPA1* and transcribed *in vitro* as described above. The DNA template for crRNA synthesis was assembled by PCR using a forward primer containing the T7 promoter and the target sequence, and a reverse primer containing the reverse complement of the target sequence and the non-variable region of crRNA. The dsDNA repair template was amplified by PCR from a plasmid encoding the mNG sequence using two primers containing the 90 bp left and right homology arm sequence, respectively. Electroporation of Cpf1/crRNA and the repair template was conducted similarly to for the Cas9/sgRNA condition described above, with a modification in the electroporation solution. A.s.Cpf1 Ultra (1 µM, IDT)

and crRNA (1 µM) were pre-incubated in buffer R and mixed with RPE1 cells (0.125×10^5 cells/µl), Cpf1 electroporation enhancer (1.8 µM, IDT) and the repair template (33 nM). mNG-positive cells were sorted using FACS Aria III (BD Biosciences), equipped with 355, 405, 488, 561 and 633 nm lasers to generate a mono-allelic *HNRNPA1-mNG* clone. The knock-in clone was subjected to CRISPR-del experiments. The crRNA sequence is listed in Table S1.

CRISPR-del efficiency assessed by Flow cytometry

HNRNPA1-mNG knock-in cells were electroporated with Cas9 and the indicated sgRNA pairs for CRISPR-del application. After 8 days in culture, the cells were harvested with trypsin-EDTA solution, washed in cold PBS, and analyzed with the FACS Aria III for mNG expression. Data for more than ∼10,000 gated events were collected.

siRNA-mediated gene knockdown

Lipofectamine RNAiMAX (Thermo Fisher Scientific) was used with a final concentration of 20 nM siRNA for siRNA transfection according to manufacturer's protocol. Transfected cells were harvested at 72 h after transfection for western blotting. Control siRNA (4390843) and CEP128 siRNA pool (L-032761-02) were purchased from Life Technologies and Dharmacon, respectively.

Western blotting

Cells were lysed on ice in lysis buffer [20 mM Tris-HCl, pH 7.5, 50 mM NaCl, 1% Triton X-100, 5 mM EGTA, 1 mM DTT, 2 mM $MgCl_2$ and 1:1000 protease inhibitor cocktail (nacalai tesque)]. After centrifugation (16,100 ***g*** for 10 min), the supernatant was added to Laemmli sample buffer, boiled and subjected to SDS-PAGE. Separated proteins were transferred onto Immobilon-P membrane (Merck) using Trans-Blot SD Semi-Dry Electrophoretic Transfer Cell (Bio-Rad Laboratories). The membranes were probed with the primary antibodies (see below), followed by incubation with their respective HRP-conjugated secondary antibodies (Promega). The membrane was soaked with Chemi-Lumi Super (Nacalai Tesque) for the signal detection using ChemiDoc XRS+ (Bio-Rad Laboratories). Images of full western blots are shown in Fig. S5.

Immunofluorescence

For the immunofluorescence analyses, cells cultured on coverslips (Matsunami) were fixed with −20°C methanol for 7 min, or 4% PFA at room temperature for 30 min. Fixed cells were incubated with blocking buffer (1% bovine serum albumin in PBS containing 0.05% Triton X-100) for 30 min at room temperature. The cells were then incubated with primary antibodies (see below) in the blocking buffer for 1 h in a humid chamber. After washing with PBS, the cells were incubated with secondary antibodies and Hoechst 33258 (DOJINDO, 1:3000–1:5000) in the blocking buffer for 30 min, followed by a final wash with PBS. The coverslips were mounted onto glass slides (Matsunami) using ProLong Gold Antifade Mountant (Molecular Probes), with the cell side down. Images were acquired as *z*-stacks with an AxioImager M2 fluorescence microscope (Carl Zeiss) equipped with a 63×/1.4 or 40×/1.3 NA objective lens. The fluorescence intensity of centrosomal proteins was measured from the maximum projection images using FIJI (National Institutes of Health, Bethesda, MD, USA). The mean fluorescence intensity of a fixed-size area around the centrosome was calculated. The measurement was corrected for background intensity by subtracting the cytoplasmic signal within the same size area near the centrosome.

Antibodies

The following primary antibodies were used in this study: anti-CEP128 [Abcam, ab118797; immunofluorescence (IF) 1:500, western blotting (WB) 1:1000], anti-γ-tubulin (Merck, GTU88; IF 1:1000), anti-p15 (Santa Cruz Biotechnology, sc-271791; WB 1:1000), anti-centrin (Millipore, A302-479A; IF 1:1000), anti-KLC1 (Abcam, ab187179; IF 1:500), anti-HSP90 (BD Biosciences, 610419; WB 1:1000) and anti-β-actin (Santa Cruz Biotechnology, sc-47778; WB 1:1000). The following secondary antibodies were used: anti-mouse IgG Alexa Fluor 488 (Molecular Probes, 1:1000), anti-rabbit IgG Alexa Fluor 555 (Molecular Probes, 1:1000), anti-mouse IgG HRP (Promega, WB 1:10,000) and anti-rabbit IgG HRP (Promega, WB 1:10,000).

T7E1 assay

Cas9/sgRNA RNPs were electroporated into RPE1 cells as described above. After 3 days in culture, their genomic DNA was purified using NucleoSpin DNA RapidLyse kit. The genomic region containing the CRISPR target site was PCR amplified, and the products were purified using a QIAquick Gel Extraction Kit (QIAGEN) and then subjected to a re-annealing process to enable heteroduplex formation. After re-annealing, the products were treated with T7 Endonuclease I (New England Biolabs) and the reaction was stopped by adding 0.25 M EDTA. The reaction product was purified using AMPure^{TM} XP (Agencourt, Beckmann- Coulter) and analyzed by agarose gel electrophoresis.

Statistical analysis

Statistical comparison between the data from different groups was performed in PRISM v.9 software (GraphPad Software) using either a Mann–Whitney *U* test or a Tukey–Kramer test as indicated in the figure legend. $P<0.05$ was considered statistically significant. All data shown are mean±s.d. No statistical method was used to predetermine the sample size. The sample size is indicated in the figure legends.

Acknowledgements

We thank the Kitagawa lab members and Dr Elmar Schiebel from ZMBH in Heidelberg University for technical supports and helpful discussions.

Competing interests

The authors declare no competing or financial interests.

Author contributions

Conceptualization: S.H.; Methodology: T.K., A.M., M.G.; Validation: T.K., A.M., T.H.; Formal analysis: T.K., S.H.; Investigation: T.K.; Data curation: T.K.; Writing - original draft: S.H., D.K.; Writing - review & editing: S.H., M.F., T.C., D.K.; Visualization: T.K.; Supervision: S.H., D.K.; Project administration: S.H., D.K.; Funding acquisition: S.H., M.F., T.C., D.K.

Funding

This work was supported by Japan Society for the Promotion of Science (JSPS) KAKENHI grants (Grant numbers: 18K06246, 19H05651, 20K15987, 20K22701, 21H02623, 22J23549, 22H02629, 22K19305, 22K19370) from the Ministry of Education, Science, Sports and Culture of Japan, the PRESTO program (JPMJPR21EC) and the CREST program (JPMJCR22E1) of the Japan Science and Technology Agency, Takeda Science Foundation, The Uehara Memorial Foundation, The Research Foundation for Pharmaceutical Sciences, Koyanagi Foundation, The Kanae Foundation for the Promotion of Medical Science, Kato Memorial Bioscience Foundation, Tokyo Foundation for Pharmaceutical Sciences, The Naito Foundation, Mochida Memorial Foundation for Medical and Pharmaceutical Research, and The Sumitomo Foundation. Open access funding provided by the University of Tokyo. Deposited in PMC for immediate release.

Data availability

All relevant data can be found within the article and its supplementary information.

Peer review history

The peer review history is available online at https://journals.biologists.com/jcs/lookup/doi/10.1242/jcs.260000.reviewer-comments.pdf

References

Bagheri, A., Culp, P. A., Dubridge, R. B. and Chen, T. T. (2022). CRISPR/Cas9 disruption of EpCAM Exon 2 results in cell-surface expression of a truncated protein targeted by an EpCAM specific T cell engager. *Biochem. Biophys. Rep.* **29**, 101205. doi:10.1016/j.bbrep.2022.101205

Baker, M. J., Goldstein, A. M., Gordon, P. L., Harbaugh, K. S., Mackley, H. B., Glantz, M. J. and Drabick, J. J. (2016). An interstitial deletion within 9p21.3 and extending beyond CDKN2A predisposes to melanoma, neural system tumours and possible haematological malignancies. *J. Med. Genet.* **53**, 721-727. doi:10.1136/jmedgenet-2015-103446

Beroukhim, R., Mermel, C. H., Porter, D., Wei, G., Raychaudhuri, S., Donovan, J., Barretina, J., Boehm, J. S., Dobson, J., Urashima, M. et al.

(2010). The landscape of somatic copy-number alteration across human cancers. *Nature* **463**, 899-905. doi:10.1038/nature08822

Biamonti, G., Bassi, M. T., Cartegni, L., Mechta, F., Buvoli, M., Cobianchi, F. and Riva, S. (1993). Human hnRNP protein A1 gene expression: structural and functional characterization of the promoter. *J. Mol. Biol.* **230**, 77-89. doi:10.1006/jmbi.1993.1127

Bignell, G. R., Greenman, C. D., Davies, H., Butler, A. P., Edkins, S., Andrews, J. M., Buck, G., Chen, L., Beare, D., Latimer, C. et al. (2010). Signatures of mutation and selection in the cancer genome. *Nature* **463**, 893-898. doi:10.1038/nature08768

Canver, M. C., Bauer, D. E., Dass, A., Yien, Y. Y., Chung, J., Masuda, T., Maeda, T., Paw, B. H. and Orkin, S. H. (2014). Characterization of genomic deletion efficiency mediated by clustered regularly interspaced palindromic repeats (CRISPR)/cas9 nuclease system in mammalian cells. *J. Biol. Chem.* **289**, 21312-21324. doi:10.1074/jbc.M114.564625

Chang, H. H. Y., Pannunzio, N. R., Adachi, N. and Lieber, M. R. (2017). Non-homologous DNA end joining and alternative pathways to double-strand break repair. *Nat. Rev. Mol. Cell Biol.* **18**, 495-506. doi:10.1038/nrm.2017.48

Concordet, J. P. and Haeussler, M. (2018). CRISPOR: Intuitive guide selection for CRISPR/Cas9 genome editing experiments and screens. *Nucleic Acids Res.* **46**, W242-W245. doi:10.1093/nar/gky354

Dewitt, M. A., Magis, W., Bray, N. L., Wang, T., Berman, J. R., Urbinati, F., Heo, S. J., Mitros, T., Muñoz, D. P., Boffelli, D. et al. (2016). Selection-free genome editing of the sickle mutation in human adult hematopoietic stem/progenitor cells. *Sci. Transl. Med.* **8**, 360ra134. doi:10.1126/scitranslmed.aaf9336

Doudna, J. A. and Charpentier, E. (2014). The new frontier of genome engineering with CRISPR-Cas9. *Science* **346**, 1258096. doi:10.1126/science.1258096

Frigerio, S., Disciglio, V., Manoukian, S., Peissel, B., Della Torre, G., Maurichi, A., Collini, P., Pasini, B., Gotti, G., Ferrari, A. et al. (2014). A large de novo 9p21.3 deletion in a girl affected by astrocytoma and multiple melanoma. *BMC Med. Genet.* **15**, 59. doi:10.1186/1471-2350-15-59

Hata, S., Pastor Peidro, A., Panic, M., Liu, P., Atorino, E., Funaya, C., Jäkle, U., Pereira, G. and Schiebel, E. (2019). The balance between KIFC3 and EG5 tetrameric kinesins controls the onset of mitotic spindle assembly. *Nat. Cell Biol.* **21**, 1138-1151. doi:10.1038/s41556-019-0382-6

He, Z., Proudfoot, C., Mileham, A. J., Mclaren, D. G., Whitelaw, C. B. A. and Lillico, S. G. (2015). Highly efficient targeted chromosome deletions using CRISPR/Cas9. *Biotechnol. Bioeng.* **112**, 1060-1064. doi:10.1002/bit.25490

Hsu, P. D., Lander, E. S. and Zhang, F. (2014). Development and applications of CRISPR-Cas9 for genome engineering. *Cell* **157**, 1262-1278. doi:10.1016/j.cell.2014.05.010

Jinek, M., Chylinski, K., Fonfara, I., Hauer, M., Doudna, J. A. and Charpentier, E. (2012). A programmable dual-RNA – guided DNA endonuclease in adaptive bacterial immunity. *Science* **337**, 816-821. doi:10.1126/science.1225829

Kim, S., Kim, D., Cho, S. W., Kim, J. and Kim, J. S. (2014). Highly efficient RNA-guided genome editing in human cells via delivery of purified Cas9 ribonucleoproteins. *Genome Res.* **24**, 1012-1019. doi:10.1101/gr.171322.113

Li, D., Sun, X., Yu, F., Perle, M. A., Araten, D. and Boeke, J. D. (2021). Application of counter-selectable marker PIGA in engineering designer deletion cell lines and characterization of CRISPR deletion efficiency. *Nucleic Acids Res.* **49**, 2642-2654. doi:10.1093/nar/gkab035

Liang, X., Potter, J., Kumar, S., Zou, Y., Quintanilla, R., Sridharan, M., Carte, J., Chen, W., Roark, N., Ranganathan, S. et al. (2015). Rapid and highly efficient mammalian cell engineering via Cas9 protein transfection. *J. Biotechnol.* **208**, 44-53. doi:10.1016/j.jbiotec.2015.04.024

Mazo, G., Soplop, N., Wang, W. J., Uryu, K. and Tsou, M. F. B. (2016). Spatial control of primary ciliogenesis by subdistal appendages alters sensation-associated properties of Cilia. *Dev. Cell* **39**, 424-437. doi:10.1016/j.devcel.2016.10.006

Meraldi, P. (2019). Bub1—the zombie protein that CRISPR cannot kill. *EMBO J.* **38**, e101912. doi:10.15252/embj.2019101912

Mou, H., Smith, J. L., Peng, L., Yin, H., Moore, J., Zhang, X. O., Song, C. Q., Sheel, A., Wu, Q., Ozata, D. M. et al. (2017). CRISPR/Cas9-mediated genome editing induces exon skipping by alternative splicing or exon deletion. *Genome Biol.* **18**, 4-11. doi:10.1186/s13059-017-1237-8

Nickerson, M. L., Witte, N., Im, K. M., Turan, S., Owens, C., Misner, K., Tsang, S. X., Cai, Z., Wu, S., Dean, M., Costello, J. C. and Theodorescu, D. (2017). Molecular analysis of urothelial cancer cell lines for modeling tumor biology and drug response. *Oncogene* **36**, 35-46. doi:10.1038/onc.2016.172

Popp, M. W. and Maquat, L. E. (2016). Leveraging rules of nonsense-mediated mRNA decay for genome engineering and personalized medicine. *Cell* **165**, 1319-1322. doi:10.1016/j.cell.2016.05.053

Raaijmakers, J. A. and Medema, R. H. (2019). Killing a zombie: a full deletion of the BUB 1 gene in HAP 1 cells. *EMBO J.* **38**, e102423. doi:10.15252/embj.2019102423

Ran, F. A., Hsu, P. D., Wright, J., Agarwala, V., Scott, D. A. and Zhang, F. (2013). Genome engineering using the CRISPR-Cas9 system. *Nat. Protoc.* **8**, 2281-2308. doi:10.1038/nprot.2013.143

Rodriguez-Rodriguez, J. A., Lewis, C., Mckinley, K. L., Sikirzhytski, V., Corona, J., Maciejowski, J., Khodjakov, A., Cheeseman, I. M. and Jallepalli, P. V. (2018). Distinct roles of RZZ and Bub1-KNL1 in mitotic checkpoint signaling and kinetochore expansion. *Curr. Biol.* **28**, 3422-3429.e5. doi:10.1016/j.cub.2018.10.006

Rouet, P., Smih, F. and Jasin, M. (1994). Introduction of double-strand breaks into the genome of mouse cells by expression of a rare-cutting endonuclease. *Mol. Cell. Biol.* **14**, 8096-8106. doi:10.1128/mcb.14.12.8096-8106.1994

Sasaki, S., Kitagawa, Y., Sekido, Y., Minna, J. D., Kuwano, H., Yokota, J. and Kohno, T. (2003). Molecular processes of chromosome 9p21 deletions in human cancers. *Oncogene* **22**, 3792-3798. doi:10.1038/sj.onc.1206589

Shalem, O., Sanjana, N. E. and Zhang, F. (2015). High-throughput functional genomics using CRISPR-Cas9. *Nat. Rev. Genet.* **16**, 299-311. doi:10.1038/nrg3899

Soheili-Nezhad, S. (2017). Alzheimer's disease: the large gene instability hypothesis. *bioRxiv* 189712. doi:10.1101/189712

Tuladhar, R., Yeu, Y., Tyler Piazza, J., Tan, Z., Rene Clemenceau, J., Wu, X., Barrett, Q., Herbert, J., Mathews, D. H., Kim, J. et al. (2019). CRISPR-Cas9-based mutagenesis frequently provokes on-target mRNA misregulation. *Nat. Commun.* **10**, 4056. doi:10.1038/s41467-019-12028-5

Xiao, A., Wang, Z., Hu, Y., Wu, Y., Luo, Z., Yang, Z., Zu, Y., Li, W., Huang, P., Tong, X. et al. (2013). Chromosomal deletions and inversions mediated by TALENs and CRISPR/Cas in zebrafish. *Nucleic Acids Res.* **41**, e141. doi:10.1093/nar/gkt781

Xu, C., Zhang, J. and Xia, X. (2020). Mammalian alternative translation initiation is mostly nonadaptive. *Mol. Biol. Evol.* **37**, 2015-2028. doi:10.1093/molbev/msaa063

Zhang, G., Kruse, T., Guasch Boldú, C., Garvanska, D. H., Coscia, F., Mann, M., Barisic, M. and Nilsson, J., (2019). Efficient mitotic checkpoint signaling depends on integrated activities of Bub1 and the RZZ complex. *EMBO J.* **38**, e100977. doi:10.15252/embj.2018100977